Rare Metal Materials and Engineering
Volume 49, Issue 8, August 2020
Available online at www.rmme.ac.cn

Science Press

Cite this article as: Rare Metal Materials and Engineering, 2020, 49(8): 2658-2664.

ARTICLE

Study of the Properties of $ZrCo_{0.8}M_{0.2}$ (*M*=Co, Cu, Cr, Mn, Al) Alloys for Tritium Storage

Lv Lijun[1], Cheng Honghui[2], Qian Yuan[1], Yang Guo[1,3], Li Xiaolin[1], Wu Shengwei[1], Han Xingbo[1], Liu Wei[1]

[1] Shanghai Institute of Applied Physics, Chinese Academy of Sciences, Shanghai 201800, China; [2] Yangzhou University, Yangzhou 225127, China; [3] University of Chinese Academy of Sciences, Beijing 100049, China

Abstract: $ZrCo_{0.8}M_{0.2}$ (*M*=Co, Cu, Cr, Mn, Al) alloys were prepared via the arc melting method in an argon atmosphere. The major phase of the alloys is ZrCo structure. The partial addition of Cr, Mn, and Al leads to the formation of a secondary phase. The Zr_2Co and $ZrCr_2$ phases, the Zr_2Co and $ZrMn_2$ phases, and the Zr_3Co and Zr_6CoAl_2 phases are formed upon Cr, Mn, and Al substitution, respectively. The cell volume of the alloys decreases upon the Cr and Mn substitution, but increases upon the Cu and Al replacement. Moreover, the hydrogen storage capacity of the alloys decreases when Cu, Cr, Mn, or Al are present in the alloy. However, the plateau of the desorption pressure remains nearly unchanged for all the alloys. The ZrCo alloy activation performance drastically improves upon Cr and Mn addition at room temperature. The disproportionation reaction rate of $ZrCo_{0.8}M_{0.2}$ alloy decreases, due to the decrease in its driving force. A modification of the $8f_2$ and 8e sites results in a change in the disproportionation driving force in all the investigated alloys.

Key words: ZrCo alloy; phase structure; hydrogen storage property; disproportionation

ZrCo alloy is considered a suitable candidate material to replace U in tritium transport, storage, and pumping[1]. In contrast to U, ZrCo shows important properties, such as non-pyrophoricity, a low absorption equilibrium pressure, a high hydrogen storage capacity, and the ability of trapping ^3He, which is released when tritium decays[2]. Moreover, ZrCo is a non-radioactive material. However, investigations showed that ZrCo induces hydrogen disproportionation during the hydrogen absorption-desorption cycles under the presence of high hydrogen pressure and temperature[3-6]. The hydrogen induced disproportionation reaction of ZrCo can be described as follows:

$$2ZrCo + H_2 \rightarrow ZrCo_2 + ZrH_2 \quad (1)$$

From this reaction two products are formed: (1) a $ZrCo_2$ phase, which does not absorb hydrogen and (2) a ZrH_2 hydride phase, which requires a high temperature (>973 K) to release the absorbed hydrogen gas. This implies that a significant amount of hydrogen is trapped within the alloy and this causes a decrease in the ZrCo hydrogen storage capacity. Therefore, it is necessary to improve the durability of ZrCo against the hydrogen-induced disproportionation effect. Nowadays, several studies have been performed to improve the ZrCo durability against disproportionation. The substitution of the third or of the fourth element in ZrCo alloys was used for this purpose[7-11]. Jat et al[11] have studied the effects of Ni substitution on the hydrogen storage behavior of ZrCo alloys. Their results reveal that the durability against disproportionation of ZrCo-based alloys increases upon the increase of the Ni content. Zhang et al[12] experimentally investigated the thermal stability and the hydrogen storage properties of ZrCo-based alloys doped with Ti, Ni, Sc, and Fe. Their findings illustrate that the $Zr_{0.8}Ti_{0.2}Co$ alloy shows the best anti-disproportionation performance among the investigated compounds. Wan et al[13] and Jat et al[14] found that the

Received date: August 25, 2019
Foundation item: National Natural Science Foundation of China (11705266, 11575104); Natural Science Foundation of Shanghai (16ZR1443500)
Corresponding author: Han Xingbo, Ph. D., Associate Professor, Shanghai Institute of Applied Physics, Chinese Academy of Sciences, Shanghai 201800, P. R. China, Tel: 0086-21-39194359, E-mail: hanxingbo@sinap.ac.cn

hydrogen absorption/desorption cyclic stability of ZrCo-based alloys drastically improves upon the substitution of Co with Ni and Fe. This may be attributed to a higher durability against disproportionation for this set of alloys. Bekris et al[15] discussed the mechanism of hydrogen-induced disproportionation in ZrCo alloys. They assumed that the disproportionation driving force in ZrCo alloys may be attributed to the hydrogen occupation (of about 4%) of the $8f_2$ and 8e sites, which are known to be the least stable sites in the structure. This observation implies that, by replacing Zr or Co with a different element, the anti-disproportionation performance of ZrCo alloys may be improved. Based on these results, alloys doped with Cu, Cr, Mn, and Al are investigated in order to evaluate the anti-disproportionation performance of ZrCo alloys. Moreover, the effects of Cu, Cr, Mn, and Al substitutions on their hydrogen storage properties are here experimentally analyzed and discussed.

1 Experiment

$ZrCo_{0.8}M_{0.2}$ (M=Co, Cu, Cr, Mn, Al) alloys were prepared in an arc furnace under an argon atmosphere. In order to produce a homogeneous alloy, high purity Zr, Co, Cu, Mn, Cr, and Al metals were melted five times in a well-defined stoichiometric amount. The purity of the metals was 99.7%, 99.95%, 99.99%, 99.7%, 99.9%, and 99.99%, respectively. The ingots were ground mechanically into powder and their structure was determined via X-ray diffraction (XRD) by measuring the Cu Kα line. The phase abundance and the lattice parameters of the alloys were calculated via the Topas software. A thermal analysis was carried out by a differential scanning calorimeter (NETZSCH STA 449F3). The experiments were performed in the temperature range from room temperature up to 1173 K at a constant heating rate of 10 K/min and in an argon atmosphere (99.999%) with a purge rate of 20 mL/min. The desorption pressure composition (*P-C*) isotherms of the ZrCo-based alloys were obtained by employing a volumetric technique on Sieverts apparatus and using commercially available hydrogen gas with purity of 99.999%. The mathematical expression of the capacity of the hydrogen absorbed by the alloys can be formulated according to the pressure change of the system. About 1 g of sample was loaded into the reaction chamber and the apparatus was evacuated to the pressure of 10^{-4} Pa at a temperature of 773 K. The reaction was initiated by introducing in the system the hydrogen gas at room temperature and at a pressure of 100 kPa. After several absorption/desorption cycles, the hydrogen absorption capacity of the alloys saturated and the sample was considered to be fully activated. Subsequently, the hydrogen desorption *P-C* isotherms were measured at 528, 563, and 598 K. The measurement principle and the methods used to obtain the *P-C* isotherms were described in previous literature[16,17]. The hydrogen-induced disproportionation kinetics data for the alloys were measured by Sieverts-type apparatus. The measurement process consisted of the following steps: (1) the hydrogen gas was introduced into the system at room temperature, (2) upon reaching the hydrogen saturation adsorption threshold in the samples, the system was evacuated to 100 Pa, and (3) the reaction vessel was heated to a temperature between 737 and 893 K to trigger the alloy decomposition. This fixed temperature was maintained for a specific period of time. Moreover, during the entire time of the experiment, the hydrogen pressure was monitored to observe the disproportionation trend following a pressure change.

2 Results and Discussion

2.1 Alloy phases and crystal structure

The XRD patterns of the $ZrCo_{0.8}M_{0.2}$ (M=Co, Cu, Cr, Mn, Al) alloys are shown in Fig.1. The ZrCo single phase with a CsCl-type cubic structure can be formed both in the ZrCo and $ZrCo_{0.8}Cu_{0.2}$ alloy. However, for $ZrCo_{0.8}Cr_{0.2}$, $ZrCo_{0.8}Mn_{0.2}$, and $ZrCo_{0.8}Al_{0.2}$, a major phase, which constitutes the ZrCo phase with some traces of a second phase, can be identified. While the Zr_2Co and $ZrCr_2$ phases are formed upon Cr substitution, the Zr_2Co and $ZrMn_2$ phases are generated upon Mn substitution, and the Zr_3Co and Zr_6CoAl_2 phases formed upon Al replacement. Harris et al[18] reported that obtaining a single phase of ZrCo is extremely challenging and their results indicated that this process is always accompanied by the formation of $ZrCo_2$ phase. In this work, the Rietveld refinement of the XRD data was used to determine the phase abundance and the lattice parameters via the Topas software. The structural characteristics of the alloys are shown in Table 1. The data indicate that the cell volume of the alloys decreases upon the Cr and Mn substitution but increases upon Cu and Al replacement. In this study, the investigated ZrCo cell volume is slightly larger when compared to other experiments[11]. This may be caused by changes of the lattice defects and the strains in as-cast alloy, when compared to annealed one.

Fig.2 shows the XRD patterns of the investigated alloys after hydrogenation. This measurement reveals that the major

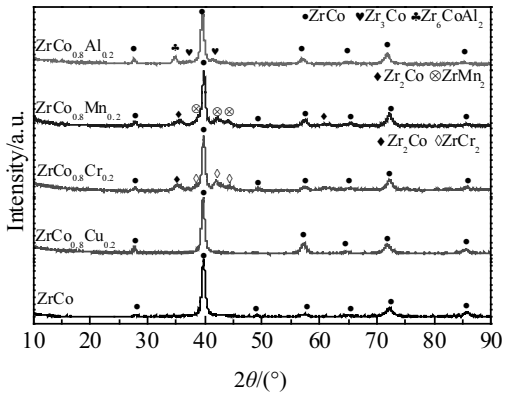

Fig.1 XRD patterns of the $ZrCo_{0.8}M_{0.2}$ alloys

Table 1 Lattice constants and phase abundances of the $ZrCo_{0.8}M_{0.2}$ alloys

Alloys	Phase	a/×10^{-1} nm	b/×10^{-1} nm	c/×10^{-1} nm	V/×10^{-3} nm^3	Phase abundance/wt%
ZrCo R_{wp}=7.59%, S=2.0	ZrCo	3.2065	-	-	32.9681	100.00
$ZrCo_{0.8}Cu_{0.2}$ R_{wp}=5.61%, S=2.4	ZrCo	3.2163	-	-	33.2702	100.00
$ZrCo_{0.8}Cr_{0.2}$ R_{wp}=4.39%, S=2.3	ZrCo	3.2019	-	-	32.8263	55.90
	Zr_2Co	6.4586	-	5.4155	225.899	21.67
	$ZrCr_2$	7.0934	-	-	356.907	22.43
$ZrCo_{0.8}Mn_{0.2}$ R_{wp}=3.96%, S=1.6	ZrCo	3.2016	-	-	32.8195	65.25
	Zr_2Co	6.4879	-	5.2682	221.758	18.38
	$ZrMn_2$	5.0313	-	8.2368	180.571	24.13
$ZrCo_{0.8}Al_{0.2}$ R_{wp}=5.45%, S=2.2	ZrCo	3.2196	-	-	33.3737	75.29
	Zr_3Co	3.3556	11.2188	8.6793	326.743	19.14
	Zr_6CoAl_2	7.9340	-	3.3928	184.958	5.56

Note: R_{wp}-weighted pattern factor, S-goodness of fit

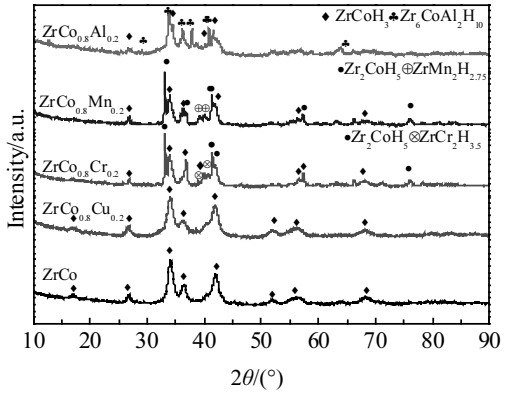

Fig.2 XRD patterns of the $ZrCo_{0.8}M_{0.2}$ alloys after hydrogenation

phase of the samples consists of $ZrCoH_3$. Moreover, the entire second phase is a hydrogen-absorbable phase. In order to gain more insights into the structure of the alloys, the lattice parameters, the cell volumes, and the phase abundance of the samples after hydrogenation were determined via the Topas software and using the Rietveld refinement method. The results are listed in Table 2. The data show that the lattice parameters and the phase abundance of the hydrogenated samples are consistent with the change in the regulation before hydrogenation. While the cell volume of the major phase increases in the $ZrCo_{0.8}Cu_{0.2}$ alloy and $ZrCo_{0.8}Al_{0.2}$ alloy, it decreases in the $ZrCo_{0.8}Cr_{0.2}$ and in the $ZrCo_{0.8}Mn_{0.2}$ alloy upon hydrogenation when compared to ZrCo.

2.2 Activation characteristics

Fig.3 presents the first activation curves of the $ZrCo_{0.8}M_{0.2}$ (M=Co, Cu, Cr, Mn, Al) alloys at $P_{initial}$=100 kPa and T=303 K. From this figure one notices that, under identical conditions, all the alloys were activated and that the maximum hydrogen capacity was obtained during the first activation. The incubation time of the first activation is element-dependent, and it decreases by following this order: Co>Cu>Al>Mn>Cr. This indicates that the activation of the alloys becomes much easier with Cr and Mn substitution. Kou et al[19] claimed that the relatively low reactivity of the ZrCo alloys may be caused by two factors: (1) the surface segregation, which is characterized by the lowest Co abundance, may be associated to a reduced catalytic activity of the Co element, and (2) the alloy surface is homogeneously covered by a ZrO_2 surface layer.

Table 2 Lattice constants and phase abundances of the $ZrCo_{0.8}M_{0.2}$ alloys after hydrogenation

Alloys	Phase	a/×10^{-1} nm	b/×10^{-1} nm	c/×10^{-1} nm	V/×10^{-3} nm^3	Abundance/wt%
ZrCo R_{wp}=3.59%, S=1.8	$ZrCoH_3$	3.5168	10.492	4.3739	161.394	100
$ZrCo_{0.8}Cu_{0.2}$ R_{wp}=5.61%, S=2.4	$ZrCoH_3$	3.5238	10.529	4.3928	162.978	100
$ZrCo_{0.8}Cr_{0.2}$ R_{wp}=6.81%, S=2.46	$ZrCoH_3$	3.5171	10.468	4.3727	160.998	64.94
	Zr_2CoH_5	6.9241	-	5.6423	270.509	18.79
	$ZrCr_2H_{3.5}$	7.5155	-	-	424.494	16.27
$ZrCo_{0.8}Mn_{0.2}$ R_{wp}=4.32%, S=1.57	$ZrCoH_3$	3.5283	10.472	4.3503	160.736	61.50
	Zr_2CoH_5	6.9309	-	5.6396	270.912	16.54
	$ZrMn_2H_{2.7}$	5.4016	-	8.8263	223.024	21.96
$ZrCo_{0.8}Al_{0.2}$ R_{wp}=6.38%, S=3.02	$ZrCoH_3$	3.4754	10.567	4.4512	163.476	58.68
	$Zr_6CoAl_2H_{10}$	8.1564	-	7.0360	405.373	41.32

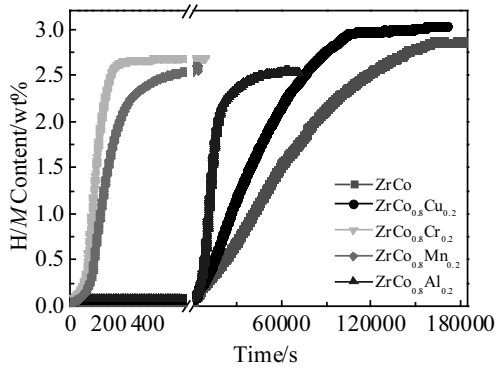

Fig.3 The first activation curves of the $ZrCo_{0.8}M_{0.2}$ (M=Co, Cu, Cr, Mn, Al) alloys at $P_{initial}$=100 kPa and T=303 K

Jacob et al[20] and Schlapbach et al[21] investigated the structure of the surface layer of the $ZrCr_2$ and $ZrMn_2$ compounds. Their results reveal that the $ZrCr_2$ local surface is composed of either ZrO_2 or of metallic chromium. The metallic chromium may contribute to the activation of the compound. Furthermore, by considering the $ZrMn_2$ case, it appears that the manganese but not the zirconium segregates and gets preferentially oxidized. The zirconium seems to form a metallic precipitate on the subsurface below the oxidized manganese. Both the precipitate and the subsurface can catalyze the H_2-2H reaction. This analysis shows that the change of the activation performance for the $ZrCo_{0.8}M_{0.2}$ alloys might be caused by the change of the surface decomposition of the alloys.

2.3 *P-C* isotherms

In order to investigate the effect of the Co substitution with other elements on the hydrogen storage properties of the ZrCo alloys, the desorption *P-C* isotherms of the alloys at the temperature of 563 K were measured. The results are reported in Fig.4. They show that there is no significant change in the desorption plateau pressure for the different ZrCo alloys. The hydrogen uptake capacity decreases with different elements in the following order: Co>Cu>Cr>Mn>Al. This may be caused by a change in the amount of the second phase. Table 1 and Table 2 show that the second phase absorbs hydrogen. Despite this evidence, the $ZrCr_2$ and the $ZrMn_2$ phases present a higher hydrogen absorption/desorption pressure[22], and they could not absorb hydrogen under the conditions reported in this study. Moreover, the Zr_2Co and the Zr_6CoAl_2 phases show a low hydrogen absorption/desorption pressure, which cannot release hydrogen. $ZrCo_{0.8}Al_{0.2}$ is composed of the lowest amount of the main $ZrCoH_3$ phase (58.68 wt%) and this results in the largest reduction in hydrogen uptake capacity[23]. However, $ZrCo_{0.8}Cu_{0.2}$ does not present any evidence of second phase and its hydrogen uptake capacity shows no significant change.

2.4 Hydrogen absorption kinetics

The hydrogen absorption kinetics for the alloys under investigation was assessed via their isothermal curves. Fig.5 shows the hydrogen absorption kinetic curves at 300 K. Under these experimental conditions, the alloys show a fast hydrogen absorption kinetics, which increases depending on the elements present in the alloy in the following order: Al>Cu>Co>Cr>Mn. Previous research suggested the fact that the lower the absorption plateau is, the larger the driving force is, which drives the hydriding process, is for an equal initial pressure. This implies that the absorption kinetics is faster[24]. Therefore, the enhanced hydrogen absorption kinetics observed may be attributed to a larger driving force in the alloys.

2.5 Hydrogen-induced disproportionation

In order to investigate the effects of Cu, Al, Mn, and Cr substitution on the hydrogen-induced disproportionation in the investigated alloys, the pressure change during the heating process at a constant temperature of 823 K was investigated. The results are shown in Fig.6. All the samples disproportionate rapidly at this temperature. Moreover, Fig.7 shows the variation of the P_t/P_0 ratio with time: P_0 and P_t represent the initial pressure and the pressure at a time t, respectively. The kinetics curves of the disproportionation for all the alloys show a Sigma-type trend, which is consistent with the results

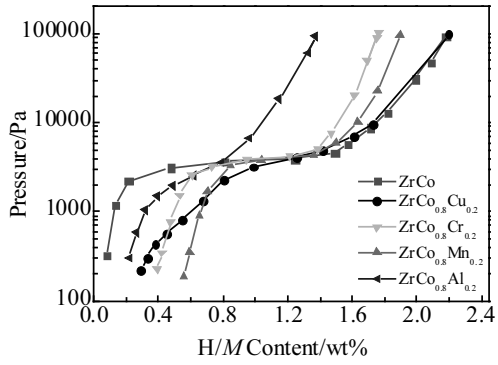

Fig.4 Desorption *P-C* isotherms of the $ZrCo_{0.8}M_{0.2}$ (M=Co, Cu, Cr, Mn, Al) alloys at 563 K

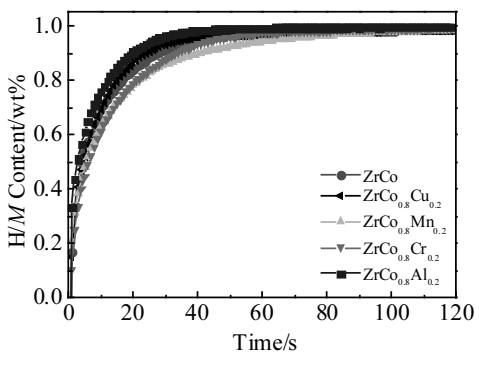

Fig.5 Hydrogen absorption kinetics of the $ZrCo_{0.8}M_{0.2}$ (M=Co, Cu, Cr, Mn, Al) alloys at 300 K

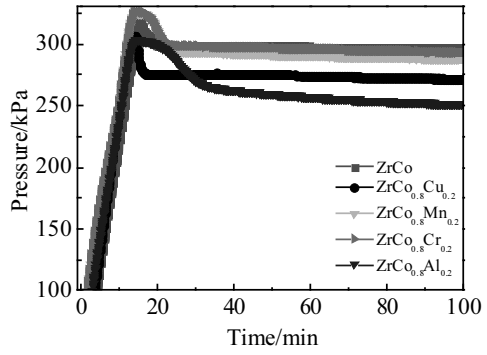

Fig.6 Kinetics of the disproportionation of the $ZrCo_{0.8}M_{0.2}$ (M=Co, Cu, Cr, Mn, Al) alloys at 823 K

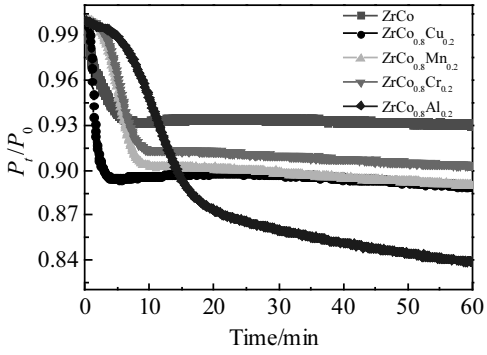

Fig.7 Normalized pressure variation of the $ZrCo_{0.8}M_{0.2}$ (M=Co, Cu, Cr, Mn, Al) alloys measured via desorption experiments at 823 K

reported in previous papers[3,25]. The disproportionation rate of the alloys is element-dependent and it decreases in the following order: Cu>Co>Mn>Cr>Al.

In order to investigate the effects of an elemental substitution on the dehydrogenation and hydrogen-induced disproportionation processes, differential scanning calorimetry (DSC) tests on the hydrides for the investigated alloys were carried out. The results are reported in Fig.8. All the samples show two hydrogen desorption peaks, which suggest that all the alloys follow a two-step hydrogen desorption process. The evolution of the hydrogen desorption peak for the low (T_1) and the high (T_2) temperature is shown in Fig.9. One notices that the trend measured at T_1 decreases in the following order: Al>Cr>Mn>Co>Cu. This trend goes in the opposite direction when compared to the evolution of the disproportionation rate. Based on the report written by Bekris[15], there exist three interstitial site types that hydrogen can occupy: (1) the $4c_1$ tetrahedral sites, which are composed of 4 Zr atoms, (2) the $4c_2$, $8f_1$, and $8g_1$ tetrahedral sites, which are composed of 3 Zr atoms and 1 Ni atom, and (3) the $8f_2$ and 8e tetrahedral sites,

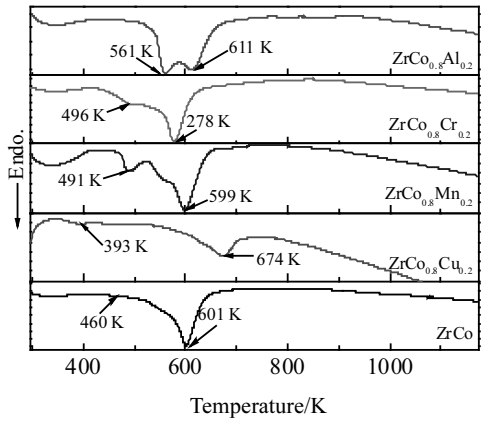

Fig.8 DSC curves of the hydrides of the $ZrCo_{0.8}M_{0.2}$ (M=Co, Cu, Cr, Mn, Al) alloys

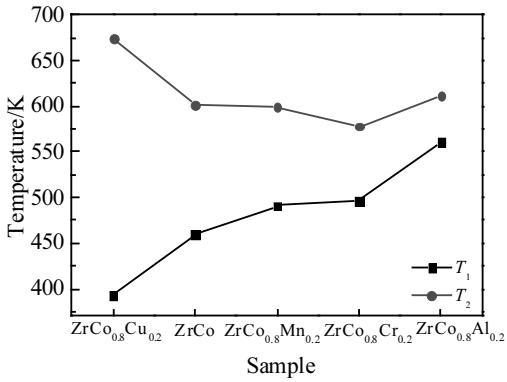

Fig.9 Comparison among the hydrogen desorption peaks for the hydrides of the $ZrCo_{0.8}M_{0.2}$ (M=Co, Cu, Cr, Mn, Al) alloys

which are composed of 2 Zr and 2 Ni atoms. Among the tetrahedral sites, the $8f_2$ and 8e sites are the least stable. They tend to form thermodynamically more stable ZrH_2 compounds, since they have a shorter Zr-H inter-distance (~0.20 nm), when compared with the ZrH_2 (~0.24 nm) compound. Moreover, the dehydrogenation process vacates the hydrogen atoms occupying the $8f_2$ and the 8e sites with partially released hydrogen from other sites. The temperature needed to vacate the hydrogen atom from an $8f_2$ or an 8e site may be considered as the first dehydriding reaction, which corresponds to the temperature T_1. In Ref. [12], the authors showed that an increase in T_1 and a decrease in the lattice parameter imply that the radius of the hole of the $8f_2$ and 8e sites decreases, and the number of hydrogen atoms occupying the $8f_2$ and 8e site decreases, preventing the generation of ZrH_2. In this research, the T_1 measured for $ZrCo_{0.8}Cr_{0.2}$ and $ZrCo_{0.8}Mn_{0.2}$ increases, whereas the lattice parameter of $ZrCo_{0.8}Cr_{0.2}$ and $ZrCo_{0.8}Mn_{0.2}$ decreases. This indicates that the

radius of the hole of the $8f_2$ and 8e sites decreases and the number of hydrogen atoms occupying the $8f_2$ and 8e sites decreases, preventing Zr-H to form ZrH_2. As a result, the disproportionation rate decreases. In the case of $ZrCo_{0.8}Cu_{0.2}$, T_1 decreases, while its lattice parameter increases, suggesting an increase in the radius of the hole of the $8f_2$ and 8e sites. The number of hydrogen atoms occupying the $8f_2$ and 8e sites increases. Thus, the tendency of Zr-H to form ZrH_2 would be promoted. The increase in the hole size of the 8e site is in agreement with Yang's conclusions[26]. For $ZrCo_{0.8}Al_{0.2}$ alloy, both T_1 and the lattice parameter increase, but the disproportionation rate decreases. Yang et al[27] concluded that the hydrogen diffusion process, the size of the 8e site, and the Zr-H (8e) bond length are three factors that affect the disproportionation of ZrCo. The decreasing disproportionation rate of $ZrCo_{0.8}Al_{0.2}$ may mainly be caused by the hydrogen diffusion process and the Zr-H (8e) bond length. Further studies are required to investigate and understand the effects of the variation in the $8f_2$ and 8e sites on the hydrogen-induced disproportionation process in ZrCo alloys upon elemental substitutions.

3 Conclusions

1) The major phase of the $ZrCo_{0.8}M_{0.2}$ (M=Co, Cu, Cr, Mn, Al) alloys presents a ZrCo structure and upon a partial substitution of Co with Cr, Mn, and Al, the formation of secondary phases (Zr_2Co and $ZrCr_2$ phases, Zr_2Co and $ZrMn_2$ phases, Zr_3Co and Zr_6CoAl_2 phases, respectively) is observed. The cell volume of the investigated alloys decreases upon Cr and Mn substitution, but increases upon Cu and Al replacement.

2) The hydrogen storage capacity of the alloys decreases upon Cu, Cr, Mn, and Al substitution, whereas the desorption plateau of the pressure of the alloys remains nearly unchanged. The activation performance of the ZrCo alloy improves effectively upon the addition of Cr and Mn at room temperature. Moreover, the hydrogen absorption kinetics of the alloys is element dependent and it increases through the following element series: Al>Cu>Co>Cr>Mn. The disproportionation rate decreases upon the addition of Cr and Mn in the alloys, due to the decrease in the driving force of this process. The change in the $8f_2$ and 8e sites in the alloys results in a change in the disproportionation driving force.

References

1 Penzhorn R D, Devillers M, Sirch M. *Journal of Nuclear Materials*[J], 1990, 170 (3): 217

2 Zhao Y M, Li R F, Tang R H *et al. Journal of Energy Chemistry*[J], 2014, 23(1): 9

3 Devillers M, Sirch M, Penzhorn R D. *Chemistry of Materials*[J], 1992, 4(3): 631

4 Hara M, Kanesaka I, Watanabe K *et al*. *Annual Report of Hydrogen Isotope Research Center, Toyama University*[J], 1994, 14: 85

5 Watanabe K, Hara M, Matsuyama M *et al. Fusion Science and Technology*[J], 1995, 28(3): 1437

6 Lu G D, Li G, Jiang G Q. *Chinese Journal of Atomic and Molecular Physics*[J], 2000, 17(1): 22 (in Chinese)

7 Huang Z, Liu X P, Jiang L J *et al. Rare Metals*[J], 2006, 25(6): 200

8 Konishi S, Nagasaki T, Okuno K *et al*. *Journal of Nuclear Materials*[J],1995, 223(3): 294

9 Tan G L, Liu X P, Jiang L J *et al*. *Transactions of Nonferrous Metals Society of China*[J], 2007, 17(S1): 949

10 Peng L X, Jiang C L, Xu Q Y *et al. Fusion Engineering Design*[J], 2013, 88(5): 299

11 Jat R A, Parida S C, Agarwal R *et al. International Journal of Hydrogen Energy*[J], 2013, 38(3): 1490

12 Zhang G H, Sang G, Xiong R J *et al. International Journal of Hydrogen Energy*[J], 2015, 40(20): 6582

13 Wan J, Li R F, Wang F *et al. International Journal of Hydrogen Energy*[J], 2016, 41(18): 7408

14 Jat R A, Singh R, Parida S C *et al. International Journal of Hydrogen Energy*[J], 2015, 40(15): 5135

15 Bekris N, Sirch M. *Fusion Science and Technology*[J], 2012, 62(1): 50

16 Cheng H H, Deng X X, Li S L *et al. International Journal of Hydrogen Energy*[J], 2007, 32(14): 3046

17 Cheng H H, Li W B, Chen W *et al. International Journal of Hydrogen Energy*[J], 2014, 39(25): 13 596

18 Harris I R, Hussain D, Barraclough K G. *Scripta Metallurgica*[J], 1970, 4(4): 305

19 Kou H Q, Luo W H, Huang Z Y *et al. International Journal of Hydrogen Energy*[J], 2016, 41(25): 10 811

20 Jacob I, Polak M. *Materials Research Bulletin*[J], 1981, 16(10): 1311

21 Schlapbach L. *Journal of the Less Common Metals*[J], 1983, 89(1): 37

22 Bloch J, Mintz M H. *Journal of Alloys and Compounds*[J], 1997, 253-254: 529

23 Bonhomme F, Yvon K, Zolliker M. *Journal of Alloys and Compounds*[J], 1993, 199(1-2): 129

24 Li S L, Cheng H H, Deng X X *et al. Journal of Alloys and Compounds*[J], 2008, 460(1-2): 186

25 Hara M, Okabe T, Mori K *et al. Fusion Engineering and Design*[J], 2000, 49-50: 831

26 Yang G, Liu W G, Han X B *et al. International Journal of Hydrogen Energy*[J], 2017, 42(24): 15 782

27 Yang G, Liu W G, Tan J *et al*. *International Journal of Hydrogen Energy*[J], 2018, 43(22): 10 410

储氚合金 $ZrCo_{0.8}M_{0.2}$ (*M*=Co, Cu, Cr, Mn, Al) 的性能研究

吕丽君[1]，程宏辉[2]，钱　渊[1]，杨　果[1,3]，李晓林[1]，吴胜伟[1]，韩兴博[1]，刘　卫[1]

(1. 中国科学院 上海应用物理研究所，上海 201800)

(2. 扬州大学，江苏 扬州 225127)

(3. 中国科学院大学，北京 100049)

摘　要：采用电弧熔炼的方法在氩气气氛中熔炼了 $ZrCo_{0.8}M_{0.2}$ (*M*=Co, Cu, Cr, Mn, Al)合金。合金的主相均为 ZrCo 相，但 Cr、Mn 和 Al 部分替代 Co 后形成了第二相。Cr 替代形成了 Zr_2Co 和 $ZrCr_2$ 相，Mn 替代形成了 Zr_2Co 和 $ZrMn_2$ 相，Al 替代形成 Zr_3Co 和 Zr_6CoAl_2 相。Cr 和 Mn 的替代使合金的晶胞体积减小，而 Cu 和 Al 的替代使晶胞体积增大。Cu、Cr、Mn 和 Al 替代后，$ZrCo_{0.8}M_{0.2}$ 合金的平台压变化不明显，但吸氢量出现了不同程度的降低。Cr 和 Mn 元素的替代明显改善了 ZrCo 合金在室温下的活化性能。Cr 和 Mn 元素的替代降低了高温下 ZrCo 合金发生歧化反应的速率，这主要是由于 Cr 和 Mn 元素的掺杂减少了氢原子占据不稳定位置 $8f_2$ 和 8e 的数量，从而降低了歧化反应发生的驱动力。

关键词：ZrCo 合金；相结构；储氢性能；歧化反应

作者简介：吕丽君，女，1988 年生，博士，中国科学院上海应用物理研究所，上海 201800，电话：021-39194997，E-mail: lvlijun@sinap.ac.cn